

Particle content of very inclined air showers for radio signal modeling

Marion Guelfand,^{a,b,*} Simon Chiche,^b Kumiko Kotera,^b Simon Prunet^{b,c} and Tanguy Pierog^d

^aSorbonne Université, CNRS, Laboratoire de Physique Nucléaire et des Hautes Energies (LPNHE), 4 Pl. Jussieu, 75005 Paris, France

^bSorbonne Université, CNRS, Institut d'Astrophysique de Paris, 98 bis bd Arago, 75014, France

^cUniversité Côte d'Azur, Observatoire de la Côte d'Azur, CNRS, Laboratoire Lagrange, Bd de l'Observatoire, CS 34229, 06304 Nice cedex 4, France

^dInstitute for Astroparticle Physics, Karlsruhe Institute of Technology (KIT), Hermann-von-Helmholtz-Platz 1, 76344 Eggenstein-Leopoldshafen, Germany
E-mail: marion.guelfand@lpnhe.in2p3.fr, simon.chiche@iap.fr, kumiko.kotera@iap.fr, simon.prunet@oca.eu, tanguy.pierog@kit.edu

The reconstruction of very inclined air showers is a new challenge for next-generation radio experiments such as the AugerPrime radio upgrade, BEACON, and GRAND, which focus on the detection of ultra-high-energy particles. To tackle it, we study the electromagnetic particle content of very inclined air showers, which has scarcely been studied so far. The features of the radio signals emitted by very inclined air showers are significantly different from those of vertical ones; in particular, they present a drastic drop of the geomagnetic emission amplitude. Using the simulation tools CORSIKA and CoREAS, and analytical modeling, we explore the energy range of the particles that contribute most to the radio emission, quantify their lateral extent, and estimate the atmospheric depth at which the radio emission is strongest. We find that the distribution of the electromagnetic component in very inclined air showers has characteristic features that could impact the reconstruction strategies of next-generation radio-detection experiments.

38th International Cosmic Ray Conference (ICRC2023)
26 July - 3 August, 2023
Nagoya, Japan



*Speaker

1. Introduction

Recently, several radio experiments (AERA, CODALEMA [1], TREND, LOFAR) have demonstrated that the information contained in the radio signal of vertical air showers allows one to perform an accurate reconstruction of the primary particle parameters (nature, arrival direction, energy). The next generation of extended radio arrays focuses on very inclined extensive air-showers (EAS) that leave large radio footprints on the ground. This specific feature allows one to deploy detectors over gigantic arrays with a sparse density to provide large detector effective area at affordable costs.

The study of the radio signal produced by these very inclined air showers has evidenced that the emission presents drastically different characteristics compared to vertical showers. In particular, the emission can become incoherent, translating into a drop in the electric field strength [2]. In order to understand the specific signatures related to this very inclined regime, we develop phenomenological models and use the Monte-Carlo simulation tools CORSIKA and CoREAS to study the leptonic content of these air-showers, directly linked to the radio signal. We examine the particle populations mainly responsible of the radio emission and the particle distribution in the shower front, taking into account shower-to-shower fluctuations.

2. Dynamics of particles for very inclined air showers

When ultra-high energy particles cross the atmosphere, they interact with air molecules and produce a cascade of secondary particles, that propagates toward the ground at relativistic speed. The electromagnetic part of the shower is responsible for the production of the radio signal: a beamed coherent emission in the MHz regime. The geomagnetic effect [3] is the major ingredient for radio emission in air: it corresponds to the deflection of electrons and positrons in opposite directions due to the Lorentz force of the Earth magnetic field, balanced by particle scattering with the air molecules. Ultimately, particles are deflected in a plane perpendicular to that of the shower propagation, creating an electric current in the atmosphere that induces a radio signal. This current varies with time since the number of electrons and positrons changes during the shower development. The emission is beamed in the forward direction inside a narrow cone due to the relativistic speed of the particles. The half-width of this cone is equal to the Cherenkov angle, typically $1\text{--}2^\circ$ in the air [4]. For an observer located at this specific angle, the radio signals emitted all along the shower arrive simultaneously, boosting the signal along this Cherenkov ring and resulting in brief and high amplitude pulses.

Very inclined air showers (with zenith angles θ larger than $\gtrsim 70^\circ$) present different geometries compared to vertical ones. They can extend over several hundreds of kilometers, as opposed to the ~ 10 km thickness of the troposphere for vertical showers. Moreover, they develop higher in the atmosphere where the air density ρ_{air} is lower (see Figure 1). This implies that shower particles have larger mean free paths for collisions with the air molecules, and hence experience more strongly the effect of the Earth magnetic field.

2.1 Scattering processes in air showers and deflections by the geomagnetic field

Electrons and positrons in the air-shower undergo Bremsstrahlung radiation at energies $\epsilon = \gamma m_e c^2 \gtrsim \epsilon_c$, where $\epsilon_c = 88$ MeV is the critical energy below which energy losses due to ion-

ization become dominant — hence most particles are absorbed in the atmosphere [5]. In terms of particle interaction processes, a transition towards multiple Coulomb scattering happens below $\epsilon_{\text{Coulomb}} = 20 \text{ MeV}$ [5]. In the following, we focus on the high energy regime where $\epsilon \gtrsim \epsilon_c$ and neglect ionization. The attenuation length for these processes can thus be written [3]:

$$l_{\text{rad}} = \frac{\epsilon^2}{\epsilon^2 + \epsilon_{\text{Coulomb}}^2} \frac{X_0}{\rho_{\text{air}}} \sim 4 \times 10^2 \text{ m} \left(\frac{\rho_{\text{air}}}{1 \text{ kg m}^{-3}} \right)^{-1} \quad (1)$$

where the numerical value assumes that the Coulomb correction factor $\epsilon^2/(\epsilon^2 + \epsilon_{\text{Coulomb}}^2) \sim 1$ and $X_0 = 36.7 \text{ g cm}^{-2}$ is the electronic radiation length.

Electrons and positrons also experience deflections in opposite directions by the geomagnetic field B , with Larmor radius $r_L \sim 3.3 \times 10^4 \text{ m} \sin \alpha (\epsilon/100 \text{ MeV})(B/10 \mu\text{T})^{-1}$, with α the so-called geomagnetic angle between the shower arrival direction and the local geomagnetic field direction.

2.2 Analytical estimate of the air-shower lateral extent

In this section, we derive an analytical estimate of the particle lateral extent at the shower front, which we define in this work as the lateral separation induced by the geomagnetic field. Assuming a continuous particle energy loss in the air, the transverse particle acceleration in the shower front at time t reads $d^2x_{\text{lat}}/dt^2 = c^3 e B \sin(\alpha)/[\epsilon_0 \exp(-t/\tau)]$, where x_{lat} is the particle transverse position (orthogonal to the shower axis), ϵ_0 is the initial energy of the particle and $\tau = l_{\text{rad}}/c$ the Bremsstrahlung energy loss timescale [3]. Integrating over time, we obtain the transverse position of particles in the shower as a function of time [2]: $x_{\text{lat}}(t) = \tau^2 c^3 e B \sin(\alpha) (e^{t/\tau} - 1 - t/\tau)/\epsilon_0$. The shower lateral extent then reads:

$$l_{\text{lat}} = 2x_{\text{lat}}(t = \tau) = 2 \left(\frac{l_{\text{rad}}}{c} \right)^2 \frac{c^3 e B (e^1 - 2)}{\epsilon_0} \sim 3 \times 10^1 \text{ m} \left(\frac{\rho_{\text{air}}}{1 \text{ kg m}^{-3}} \right)^{-2} \left(\frac{B \sin(\alpha)}{50 \mu\text{T}} \right) \left(\frac{\epsilon_0}{100 \text{ MeV}} \right)^{-1}. \quad (2)$$

where the factor 2 accounts for the dynamics of both positrons and electrons.

As demonstrated in Section 3.4, most of the emission is indeed produced in the region around the shower axis where the electron/positron density is the higher, and more specifically at X_{max} . The amplitude of the radio signal scales linearly with the number of electrons and positrons and its power scales quadratically.

If the shower lateral extent at X_{max} is larger than the spatial coherence length, the signal becomes incoherent [2].

3. Contribution of air-shower particles in radio emission

One of the first steps to link the particle content of very inclined EAS with the specific features of the radio signal consist in identifying the particles that are specifically involved in the radio

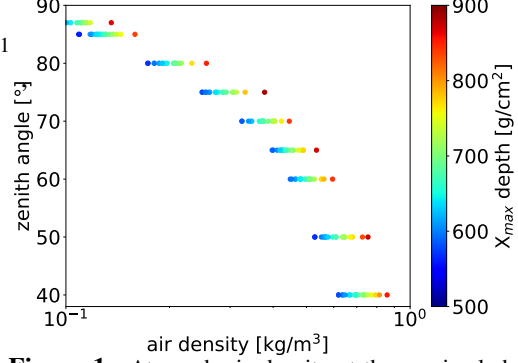


Figure 1: Atmospheric density at the maximal shower development for various inclinations. The chosen atmosphere is the U.S. standard atmosphere parametrized according to Linsley [6]. For a given inclination, the maximal shower development X_{max} position can be at different depths due to shower-to-shower fluctuations. Very inclined air-showers develop in less dense atmospheres.

emission. For this purpose, we will rely on microscopic numerical simulations.

3.1 Microscopic simulations with CORSIKA and CoREAS

We simulate air showers with CORSIKA 7.7500 [7], a detailed Monte-Carlo code which follows the individual trajectories of the particles. Quantum variations on X_{\max} , between air showers with identical primaries, are intrinsically modelled. QGSJetII is chosen as high-energy interaction model and URQMD 1.3.1 as low-energy interaction model. The primary particle is a proton with two possible energies: 10^{17} eV or 10^{18} eV, with a zenith angle between 50° and 90° and two possible azimuth angles (0° , 45°). The elevation site (1140 m) and magnetic field correspond both to those of a site close to Dunhuang, China, where the GRAND prototype is being deployed [8]. The atmosphere is approximated with the standard Linsley model [6]. We store the information on the particles of the EAS (position, energy) that cross the shower plane at X_{\max} (if no other precision) thanks to the COAST CORSIKA module.

For the radio emission computation, we use CoREAS V1.4 [9], the extension of CORSIKA that allows one to simulate the electromagnetic radiation produced by the particles of the shower. The same input parameters as CORSIKA are used, and antennas are located on the ground, on the North axis at the position where the radio signal is maximal (i.e., on the Cherenkov cone). This position is found by running simulations and recording the signal for a set of antennas on the North axis and keeping only the antenna position where the signal is maximal. The time traces obtained thanks to CoREAS are used to define the contribution of different shower stages and particle energy regimes in the emission of the radio signal.

3.2 Energy spectra of leptons in air-showers

We study the particle energy content in air showers at fixed primary energies and different arrival direction inclinations with CORSIKA simulations. We store the energy of electrons and positrons of the air-showers when they cross the shower plane (i.e., the plane perpendicular to the shower axis) at different stages of the shower development.

The energy spectra of electrons for two different zenith angles are presented in Figure 2 (Left). The colored dots and crosses indicate the total energy of particles contained in each energy bin, at a given depth of the shower for zenith angles 80° and 0° respectively. The early stages (with lower X) of the shower contain more highly energetic particles than the later stages. This feature is expected as these particles lose energy during the shower development. Furthermore, the peak region is shifted from a few tens of MeV for vertical air showers to a few hundred of MeV for very inclined air showers. This clearly appears on Figure 2 which shows the ratio of the two energy spectra in the peak energy range: more energy is contained at the critical energy for very inclined air showers.

3.3 Contribution of particle energies to radio emission

In the next step, we examine the contribution of particles of various energies to the radio signal. We run CoREAS simulations for a fixed primary with different zenith angles, and record the electromagnetic radiation emitted by the particles of the air showers in specific energy bins —i.e., in specific Lorentz factor bins— and for the whole range of energy. In Figure 3, we represent the

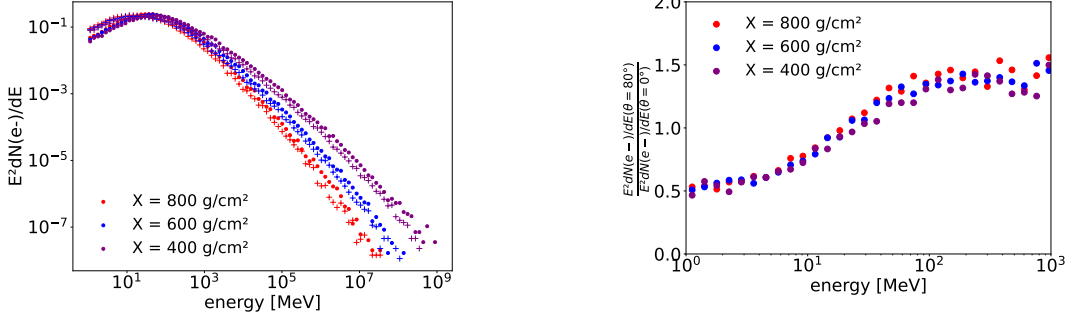


Figure 2: (Left) Electrons normalized energy spectra at different shower depths (X) and inclinations (θ). The primary particle is a proton with energy 10^{18} eV with $\theta = 0^\circ$ (crosses) and $\theta = 80^\circ$ (dots). (Right) Ratio of the very inclined ($\theta = 80^\circ$) to vertical ($\theta = 0^\circ$) electrons energy spectra.

traces of the radio signal for a zenith angle of 70° . Only the East-West polarisation of the electric field is represented, as it is largely dominant in this specific configuration: for an air shower with azimuth angle $\phi = 0^\circ$ and an antenna located on the North axis, the North-South polarization of the electric field is negligible compared to the East-West polarization.

The energy fluence, i.e., the energy deposited per area, being the time-integral of the radio pulse [10], we then integrate the electric field of each pulse over time and normalize by dividing it by the integral of the total electric field, i.e., by the sum of each integral. This enables us to compare the contribution of the different particle populations on the radio signal for each zenith angle. Figure 3 shows the mean values and uncertainties of this fraction obtained for a set of fifty simulations on each zenith angle to take into account the shower-to-shower fluctuations. It appears that the electric field is dominated by contributions from increasingly energetic particles as the inclination increases. For inclinations larger than 70° , the electric field is dominated by [50, 1500] MeV particles, which would be consistent with the energy spectra of Figure 2, peaking in this range. For showers with a lower inclination, another energy regime is dominant, in the range [10, 500] MeV.

3.4 Radio emission point in the air-shower

The contribution of different shower phases can also be estimated for air showers with different zenith angles. Following the same procedure as before, we generate with CoREAS the electric field emitted by particles with energy in the range [50, 1500] MeV or [10, 500] MeV according to the zenith angle (see Section 3.3). Comparing the fraction of the integral of the pulses that arrive at an antenna located on the Cherenkov cone as shown in Figure 4, we can see that the most representative region of the radio emission is around the maximal development of the shower X_{\max} whatever the inclination. This confirms the commonly admitted notion that the radio emission can be assumed to be produced at X_{\max} , also for very inclined air showers.

4. Particle distribution and lateral extension of very inclined air-showers

In the previous sections, we found that the energy range of the bulk of the particles is shifted at higher energies for very inclined air showers and that the shower development stage X that produces the radio signal do not vary with the zenith angle. The robustness of this last parameter can be used

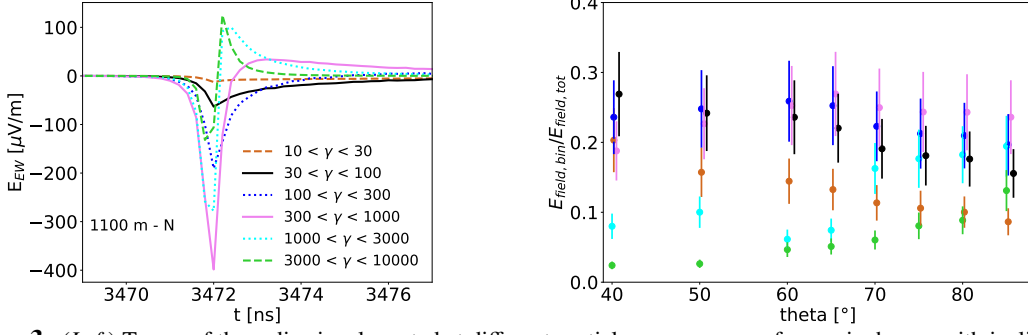


Figure 3: (Left) Traces of the radio signal created at different particle energy ranges for an air shower with inclination $\theta = 70^\circ$ and azimuth $\phi = 0^\circ$. The primary particle is a proton with energy 10^{17} eV. The antenna is located at the Cherenkov cone, at a distance of 1100 m of the shower core on the North axis. The lines represent the electric fields produced by particles in specific energy ranges as indicated. (Right) Contribution of different particle energy regimes responsible for the radio signal. Each point corresponds to the mean value of the fraction of the integral of the electric field in a given energy range on a set of 50 simulations. The error bars represent the uncertainty σ/\sqrt{N} on this value, where N is the number of simulations. The right-hand panel uses the same color code as the left one. The points and error bars have been artificially shifted for the same zenith angle for more visibility.

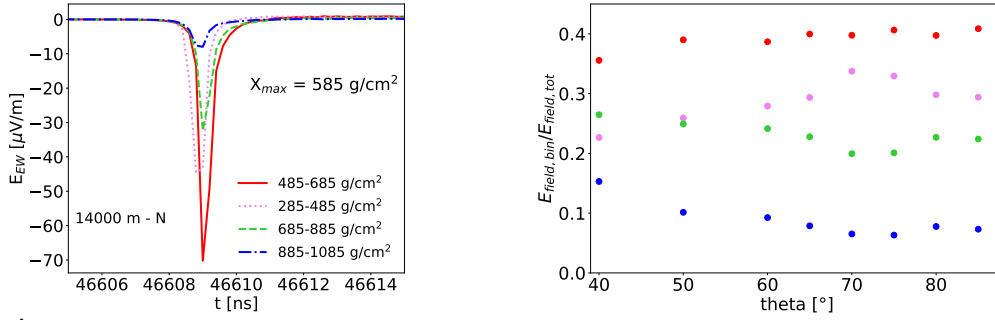


Figure 4: (Left) Traces of the radio signal created at different stages of the shower development by particles in the energy range $100 < \gamma < 3000$. The primary particle is a proton with energy 10^{17} eV, zenith angle $\theta = 85^\circ$ and azimuth $\phi = 0^\circ$. The antenna is located at the Cherenkov cone, on the North axis at a distance of 14000 m from the shower core. (Right) Contribution of shower stages in radio emission. Each point corresponds to the fraction of the integral of the electric field in a given slant depth range. For all the simulations, $X_{\max} = 585$ g/cm 2 . The right-hand panel uses the same color code as the left one.

to give a universal definition of the lateral extent of electrons and positrons in the air shower in two energy regimes depending on the inclination.

4.1 Lateral extent estimation

The spatial position of particles in the shower plane ($\mathbf{v} \times \mathbf{B}$, $\mathbf{v} \times \mathbf{v} \times \mathbf{B}$) at X_{\max} is easily accessible with CORSIKA, as shown in Figure 5, which represents the particle density contained inside ellipses in the shower plane for a zenith angle of 82° . Most of the particles are contained at the center of the shower, where most secondary particles are produced, and many electrons and positrons are deflected along the $\mathbf{v} \times \mathbf{B}$ axis, in opposite directions, due to the geomagnetic field, as mentioned in Section 2.1. To estimate the lateral extension of the particles, we therefore work on the projection of the particle positions along the $\mathbf{v} \times \mathbf{B}$ axis, as this deflection produces a time varying current mainly responsible for the radio emission. Figure 5 represents the cumulative fraction of

particle energies at fixed distances of the shower core and the corresponding particle fractions for three different inclinations. It appears that the relationship between energy fraction and particle number at a given distance is a power law whatever the zenith angle.

At the distance from the shower axis where the shower contains 90% of the particles, more than 90% of the energy is also contained. This distance is thus representative of the lateral extent and is chosen as the lateral extent estimator in this work.

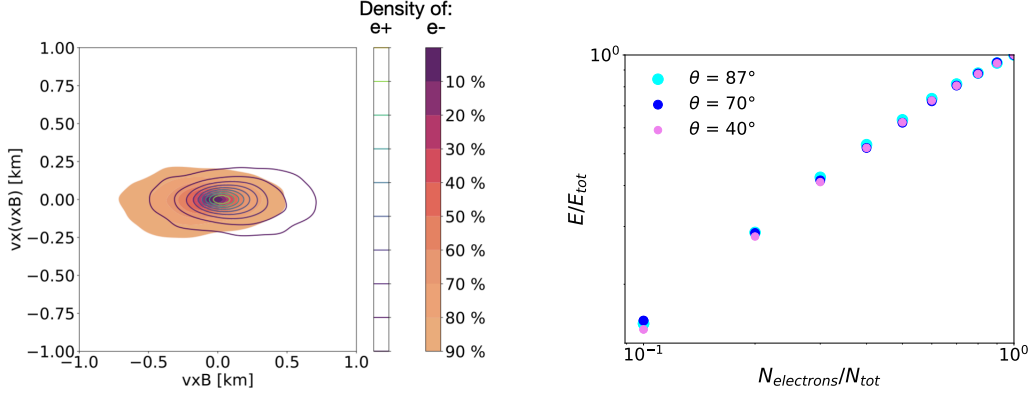


Figure 5: (Left) Electrons and positrons density inside ellipses of the shower plane at X_{\max} . The limits of the regions are defined by color contours for electrons and linear contours for positrons. Only particles in the energy range [50, 1500] MeV are represented. The primary particle is a proton with energy 10^{18} eV, inclination $\theta = 82^\circ$ and azimuth $\phi = 45^\circ$. (Right) Fraction of energy contained at fixed distance in the shower plane at X_{\max} and corresponding fraction of particles for 3 zenith angles. The distances correspond to the projection of particle positions along the $\mathbf{v} \times \mathbf{B}$ axis. For $\theta = 40^\circ$, only particles in the range [10, 500] MeV are selected, for $\theta = 82^\circ$ and $\theta = 70^\circ$, the range [50, 1500] MeV is selected.

4.2 Lateral extent as a function of inclination

The lateral extent is computed on a set of 200 simulations obtained with CORSIKA for air showers with zenith angles varying between 30° and 85° –and thus for different atmospheric densities as shown in Figure 6. According to Sections 3.2 and 3.3, the energy is function of the inclination and two different ranges of particle energies are selected: [50, 1500] MeV for particles above 70° and [10, 500] for particles below.

We observe that the lateral extent increases with zenith angle, because inclined air showers develop in thinner atmosphere than vertical ones. The black dashed line corresponds to the analytical calculation of the extension induced by the geomagnetic field, presented in Eq. (2) for an energy of 100 MeV. The corresponding particles are indeed representative of the leptonic content in very inclined air showers (see Section 3.2). The blue dotted line is the Molière radius given in Ref. [3] by $R_M = (9.6 \text{ g/cm}^2)/\rho_{\text{air}}$ which represents the spread due to scattering. Hence, two distinct regimes are highlighted at low and high inclinations: whereas

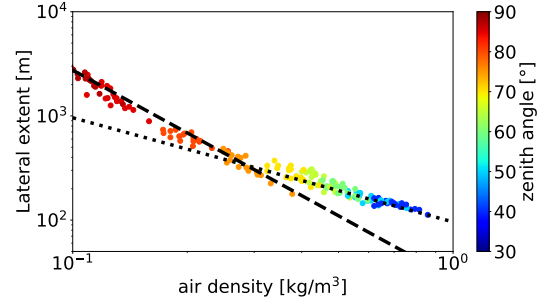


Figure 6: Lateral extent of particles in the shower plane at X_{\max} for air showers with inclinations between 30° and 85° on a set of 200 simulations. The air-density at X_{\max} is also represented. The dashed line is the analytical calculation of the lateral extent given in Section 2 and the dotted line stands for the Molière radius.

the lateral extent of vertical air-showers is driven by multiple scattering, very inclined air showers experience a drastic lateral extent increase due to the Earth's magnetic field.

5. Conclusion

Using CORSIKA and CoREAS simulations, we demonstrate the robustness of stages of the shower development that contribute to the radio emission with zenith angle. Based on this result, we constructed a global estimator of the particle lateral extent in two different energy regimes depending on the inclination. The distance to the shower axis where 90% of the particles are contained can be safely used as an estimator of the lateral extent.

Computing this estimator in our simulations, we find a drastic lateral extent increase for very inclined air showers subjected to a strong enough magnetic field, which results in a loss of coherence and in a drop of the radio signal [2]. This specific feature will strongly impact the reconstruction strategies of the next generation of extended radio arrays and could, for example, allow us to discriminate between cosmic-ray air showers and neutrinos that also have very inclined trajectories but which develop in very dense atmosphere [2].

Aknowledgments

The authors thank V. Niess and M. Tueros for their careful reading, as well as the GRAND-Paris team, T. Huege and the GRAND team at KIT for fruitful discussions. This work was supported by the Programme National des Hautes Energies of CNRS/INSU with INP and IN2P3, co-funded by CEA and CNES. Simulations were performed using the computing resources at the CCIN2P3 Computing Centre (Lyon/Villeurbanne – France), partnership between CNRS/IN2P3 and CEA/DSM/Irfu. This work is part of the NuTRIG project, supported by the Agence Nationale de la Recherche (ANR-21-CE31-0025; France) and the Deutsche Forschungsgemeinschaft (DFG; Projektnummer 490843803; Germany).

References

- [1] T. Huege *Physics Reports* **620** (Mar, 2016) 1–52.
- [2] **GRAND** Collaboration, S. Chiche *et al. PoS ICRC2023* (these proceedings) 394.
- [3] O. Scholten, K. Werner, and F. Ruydi *Astroparticle Physics* **29** no. 2, (03, 2008) 94–103.
- [4] F. G. Schröder *Progress in Particle and Nuclear Physics* **93** (03, 2017) 1–68.
- [5] T. K. Gaisser, R. Engel, and E. Resconi, *Cosmic Rays and Particle Physics*. 2016.
- [6] A. M. Hillas **22** (Jan., 1984) 425–444.
- [7] D. Heck, J. Knapp, J. N. Capdevielle, G. Schatz, and T. Thouw, *CORSIKA: a Monte Carlo code to simulate extensive air showers*. 1998.
- [8] **GRAND** Collaboration, J. Torres de Mello Neto *PoS ICRC2023* (these proceedings) 1050.
- [9] T. Huege, M. Ludwig, and C. W. James, “Simulating radio emission from air showers with CoREAS,” in *AIP Conference Proceedings*. AIP, 2013. <https://doi.org/10.1063%2F1.4807534>.
- [10] C. Glaser, M. Erdmann, J. R. Hörandel, T. Huege, and J. Schulz *Journal of Cosmology and Astroparticle Physics* **2016** no. 09, (Sep, 2016) 024–024.